(A New Proposal to Jefferson Lab PAC25)

High resolution study of the 1540 exotic state

J. P. Chen, E. Chudakov, C. DeJager, P. Degtyarenko, R. Feuerbach, M. Jones, J. Gomez, O. Hansen, D. W. Higinbotham, J. LeRose, W. Melnitchouk, R. Michaels, S. Nanda, B. Reitz, A. Saha, B. Wojtsekhowski (spokesperson)
Thomas Jefferson National Accelerator Facility, Newport News, VA 23606

G. Cates, D. Day, A. Deur, R. Lindgren, N. Liyanage, V. Nelyubin[†], B. E. Norum, J. Singh, R. Snyder, W. A. Tobias, K. Wang
University of Virginia, Charlottesville, VA 22901

P. Souder, R. Holmes, B. Hachemi
Syracuse University, Suracuse, NY 13244

K. Kumar, K. Paschke, L. Kaufman
University of Massachusets, Amherst, MA

D. Nikolenko, I. Rachek
Budker Institute, Novosibirsk, Russia

W. Briscoe, R. Arndt, I. Strakovsky, R. Workman
Center for Nuclear Studies, Department of Physics
The George Washington University, Washington DC 20052

Y. Azimov
SPNPI of Russian Academy of Science, Gatchina, Russia

M. Polyakov
Inst. de Physique au Sart-Tilman, Liege 1, Belgium

J. Annand, D. Ireland, J. Kellie, K. Livingston, G. Rosner
University of Glasgow, Glasgow, Scotland

P. Markowitz
Florida International University, Miami, FL 33199

W. Korsch
The University of Kentucky, Lexington, KY 40506

J. Calarco, W. Hersman
University of New Hampshire, Durham, NH 03824

V. Kubarovsky
RPI, Troy, NY 12180-3590 and TJNAF, Newport News, VA 23606

R. Gilman, K. McCormick
Rutgers, The State University of New Jersey, Piscataway, NJ 08854

F. Garibaldi, S. Frullani, G. M. Urciuoli, M. Iodice
INFN, Rome, Italy

E. Piasetzky
Tel Aviv University, Israel

L. Pentchev
College of William and Mary, Williamsburg, VA 23185

K. Egiyan, S. Mayilyan, V. Mamyan, A. Shahinyan
Yerevan Physics Institute, Yerevan, Armenia

† on leave from SPNPI of Russian Academy of Sciences, Gatchina, Russia

November 9, 2003

Abstract

An experiment is proposed to measure the parameters of an exotic state recently observed in the reaction n$(\gamma, K^- n K^+)$. Measurements of three closely connected reactions are proposed here.

Investigation of the first reaction D$(e, K^- n K^+)$X has the goal to measure the resonance mass and width with a resolution (FWHM) of 3.5 MeV , and an angular distribution of the decay products, which may allow determination of the spin/parity of the Θ^+.

Investigation of the second reaction D$(e, e' K^- p_{soft})$X has the goal to a measure the resonance mass and width with a resolution (FWHM) of 3.5 MeV ; learn about t dependence of the reaction cross section and Θ^+ form-factor ; and get an estimate of the photon linear polarization asymmetry, which may provide a key to Θ^+ parity.

Both measurements will measure the photo-production cross section with few percent accuracy.

Investigation of the third reaction H$(e, e' K^-)$X (and H$(e, e' K^+)$X) has the goal to search of the Θ^+ state partners, namely Θ^{++} and Σ^0.

The experiment utilizes a 4.5(6.0) GeV electron beam in Hall A, HRS spectrometers with the septum magnets, a BigBite spectrometer, and a large neutron detector. This equipment exists or is under construction for recently approved experiments. With 796 hours of beam-time for all three measurements data will be obtained on the resonance width, mass and quantum numbers.

Such measurements would dramatically increase our experimental confidence in the parameters of the exotic state and its nature.

1 Introduction

A new baryon resonance (Θ^+) in K^+n and K^o_sp systems was observed by several independent experiments [2, 3, 4, 5, 6, 7, 8]. Because of its positive strangeness the Θ^+ is explicitly exotic and its minimal quark content is $uudd\bar{s}$.

Such a state was predicted as a member of an antidecuplet of the flavor group $SU(3)_F$ [1]. This unitary identification assumes zero isospin of Θ^+, and continues to be popular [10, 11, 13]. However, other identifications with higher isospin, have also been suggested in the literature [12, 14]. They may imply existence of such relative states as Θ^{++}. Different idea on the origin of the small width was suggested in [15].

The mass of Θ^+ was predicted to equal 1530 MeV [1]. Several of the present experiments give the nearby value 1540 MeV, but some of them result in low values down to 1526 MeV (see Table 1).

Collaboration	Mass (MeV)	Width (MeV)	Ref
DPP	1530	<15	[1]
LEPS	1540±10	<25	[2]
DIANA	1539±2	<9	[3]
CLAS/γn	1542±5	<21	[4]
CLAS/γp	1540±10	<32	[5]
ELSA	1540±4±2	<25	[6]
ITEP/ν	1533±5	<20	[7]
HERMES	1526±2±2	<18	[8]
USC	1543	<3–6	[16]
GWU	1540–1550	≤1	[17]
Jülich	1545	<5	[?]

Table 1: Comparison of recent Θ^+ findings.

The spin of Θ^+ is unknown, though there are weak evidences that the spin 1/2 is preferred, as was predicted [1]. The parity predicted to be positive is totally unknown, and induced discussions in the literature since in terms of the quark structure it requires presence of a P-wave.

The most intriguing today is the width of the Θ^+. The theoretical prediction was $\Gamma_{\Theta^+} < 15$ MeV [1]. Existing experiments cannot measure Γ_{Θ^+}, however show that the width is smaller than the experimental resolution. Most experimental publications give an upper boundary of 20 MeV, larger than expected by theory. The Xenon bubble chamber data, corresponding in essence to the charge exchange $K^+n \to K^0p$, provide a slightly lower boundary of 9 MeV [3]. Less direct treatment [16], using the published data on K^+d total cross section, leads to a stronger limitation $\Gamma_{\Theta^+} < 6$ MeV. The partial-wave analysis of available KN (elastic and charge exchange) scattering data pretends to exclude even widths above 1 MeV [17]. If the width is indeed so small, it is natural to expect that other members of

the same multiplet (antidecuplet ?) should have comparable widths. Such expectation is supported by recent evidence for one more exotic state Ξ^{--} having width also less than a resolution [9].

The width on the level of few MeV will indicate that Θ^+ has very different structure than known baryons. Our primary goal will be an investigation of the actual width of the Θ^+. The key advantage of JLab Hall A apparatus is its capability to provide sub MeV energy resolution in electro/photo production of the resonance; the small angle, high momentum detection and excellent PID for few GeV kaons. Presented below ideas on detection of the soft protons and decay particles allow to complete the setup needed for study of the Θ^+. The angular distribution of decay products may allow determination of spin and parity of resonance, which is another important goal of proposed experiment.

There are two other members of possible antidecuplet which also can be observed by using the same detector system, namely Σ^- and Σ°. The Θ^{++} member of the possible isotensor multiplet also can be searched. Hall A two septum setup has very high sensitivity in the search for Σ° and Θ^{++}.

We therefore propose a search and an investigation of the exotic baryon in electromagnetic reactions from the neutron and proton.

The proposal is organized as follows. In Section 1 we present the physics motivation and the goals of the proposed experiment. In Section 2 we showed an experimental information on inclusive photo-production of the negative kaons in the diffractive regime, which allow to make an estimate of the non-resonance and accidental background in expected data. In Section 3 we describe essential features of both the standard and the specialized equipment. Section 4 presents the proposed measurements, the calculations of the mass resolution and event rates. Expected results and a beam time request are shown in Section 5. The proposal is summarized in Section 6.

2 Inclusive electro-production

In this section we are discussing the inclusive reactions, which define the singles rates of electrons, pions and kaons in the spectrometers.

In both the BigBite and the Neutron arm detectors the rates at low energy part of the particle spectra dominate. We used DINREG Monte Carlo calculations [22] for analysis of the low energy part of the inclusive spectra ($E_{hadron} << E_{beam}$). DINREG reproduced well published neutron and proton yields in electro-nuclear reactions [23] . DINREG based predictions for the wire chamber rate was found in agreement with recent measurements in Hall A [25].

The HRS-left will be used to detect negative charge particles with momentum about 3 GeV/c, where the single rate is dominated by electrons from deep inelastic scattering (DIS) and photo-produced pions. The yields of negative pions and kaons were calculated by using results from DESY and SLAC measurements of inclusive photo-production [26, 27, 28]. Similar analysis was done for the HRS-right, which will be used for detection of scattered electrons in the first and third proposed measurements.

2.1 Kinematics and definitions

The kinematics of electro-production is presented in Fig. 1.

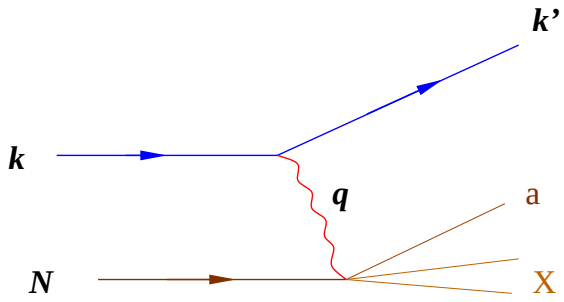

Figure 1: Kinematics quantities for description of electro-nucleon scattering. k and k' are the four-momenta of incoming and outgoing leptons, P is the four-momentum of a nucleon with mass M. The exchange photon transfers four-momentum $q = k - k'$ to the target.

The definitions of the kinematical variables are given for the reaction $e + N \rightarrow e' + a + X$. The five four-momenta involved are:

$$k = (E, \vec{k}), \text{ for the incident electron}$$
$$k' = (E', \vec{k'}), \text{ for the scattered electron}$$
$$N = (M, \vec{P}), \text{ for the target nucleon}$$
$$a = (E_a, \vec{p}_a), \text{ for the produced hadron}$$

$$X = (E_X, \vec{p}_X), \text{ for the residual system}$$

A few kinematic variables are defined below as:

$$q^2 = (k - k')^2 = -Q^2,$$
$$\nu = E - E',$$
$$\epsilon = \left[1 + 2\frac{\nu^2+Q^2}{Q^2} tan^2\frac{\theta_e}{2}\right]^{-1},$$
$$s = (q + N)^2 = W^2, \quad t = (q - N)^2,$$
$$x_B = Q^2/2M\nu, \text{ the Bjorken variable}$$
$$x_F = p^{cm}_{a,z}/p^{cm}_{a,max}, \text{ the Feynman variable}$$

The differential cross section of inelastic eN scattering processes is written in the usual notation as

$$\frac{d^2\sigma}{dE' d\Omega_{e'}} = \frac{\alpha^2}{4E^2 sin^4(\frac{\theta}{2})}\left[W_2(q^2,\nu)cos^2(\frac{\theta}{2}) + 2W_1(q^2,\nu)sin^2(\frac{\theta}{2})\right]$$

In approximation of $E, E' >> M_N$ and finite q^2, ν we will use

$$\frac{d^2\sigma}{dE' d\Omega_{e'}} \approx \frac{\alpha^2}{4E^2 sin^4(\frac{\theta}{2})}\frac{F_2(q^2,\nu)}{\nu}$$

The differential cross section for electro-production of hadron a can be presented as:

$$\frac{d^3\sigma}{dE' d\Omega_{e'} d\Omega_a} = \Gamma \cdot \frac{d\sigma_{\gamma^*,a}}{d\Omega_a},$$

where Γ is the virtual photon flux factor, given by:

$$\Gamma = \frac{\alpha}{2\pi^2}\frac{E'}{E}\frac{s-M^2}{2MQ^2}\frac{1}{1-\epsilon}$$

and $\frac{d\sigma_{\gamma^*,a}}{d\Omega_a}$ is a cross section for hadron production by the virtual photon. At small scattering angle, where $Q^2 << M^2$, only transverse terms of the cross section are contribute, so we will use the form:

$$\frac{d\sigma_{\gamma^*,a}}{d\Omega_a} = \frac{d\sigma_T}{d\Omega_a} + \epsilon\,\frac{d\sigma_{TT}}{d\Omega_a}\,cos(2\phi),$$

where ϕ is an angle between an electron scattering plane and a hadron production plane.

In an approximation of limiting fragmentation the invariant cross section $E\frac{d^3\sigma}{d^3p}$ for the production of specific hadron a is a function of x_F and $p^2_\perp$ [29]. At 6 GeV photon energy the accuracy of such approximation can be estimated on the level of 30% for large x_F and small $p^2_\perp$ [28] (see Fig. 2).

2.2 The electron single rates in HRS

In the present experiment the HRS will be at 6° and the central momentum at 2 - 3 GeV/c. The kinematics for the beam energy of 6 GeV corresponds to Q^2 of 0.1-0.2 (GeV/c)^2. The DIS cross section can be used to estimate the rate. It leads to a rate of 300-600 kHz at luminosity of 1×10^{38} Hz/cm^2. A similar estimate can be obtained as mentioned above from the total photo-production cross section and flux of the virtual photons.

spectrometer	momentum	electron rate
HRS-left	3.0 GeV/c	500 kHz
HRS-right	2.0 GeV/c	290 kHz

Table 2: The electron rates for E_{beam} = 6 GeV, $\theta_{HRSs} = 6°$, at electron-nucleon luminosity of 1×10^{38} Hz/cm^2.

2.3 The pion and kaon rates in HRS

At high beam energy the inclusive processes in the regime of large momentum of the produced hadron can be understood in the framework of hypothesis of limiting fragmentation [30, 29]. Cross sections are analyzed in terms of Feynman's variable x_F and $p_\perp^2$. The experimental results [27, 28] agreed quantitatively with quark model predictions. These data are shown in Fig. 3. For the photon energies of this proposal (4 GeV) applicability of limiting fragmentation ideas can be justified by reasonable agreement between high energy results [27, 28] and measurement at E_γ = 3.2 GeV [26]. For calculation of the particle yields the photon intensity need to be calculated. The intensity of the equivalent photon flux in electroproduction experiment was calculated according to a prescription [31]. The photon spectra are shown in Fig. 4.

The resulting counting rates are shown in the Table 3.

spectrometer	momentum	π^- rate	K$^-$ rate
HRS-left	3.0 GeV/c	150 kHz	2.5 kHz
HRS-right	2.0 GeV/c	180 kHz	10 kHz

Table 3: The π^- and K$^-$ singles rates at conditions of the Table 2.

2.4 Coinsidence rate between HRSs

In the second measurement both HRSs will be used. The coincidence between them will be used as a DAQ trigger. The rate of electron-hadron coincidence was estimated from the flux of virtual photons and hadron photo-production rate as was discribed above in this

Section. The aerogel counter in HRS will provide on-line rejection factor of 100, which allow to keep DAQ rate on acceptable level of 5 kHz (see Tab. 4).

event type	$e\pi^-$ rate	eK^- rate
rate, Hz	150	1

Table 4: The π^- and K^- coincidence rates in the HRSs at conditions of the Tab. 2. For momenta of HRS-left of 3 GeV/c and HRS-right of 2 GeV/c.

2.5 Single rate in the BigBite

The proposed configuration of the detectors was analyzed for single rates, which defined the maximum usable luminosity and possible production rate. This section deals with the calculation and measurement of the single rate in the BigBite spectrometer for both parts of proposed experiment.

Figure 5 shows the expected rate of electrons at different momenta. The proton rates are shown in Fig. 6. For cross check of these calculations we made a measurement of a counting rate of the multi-wire proportional chamber located behind BigBite at 65° on distance 8 m from the target. During measurements the beam energy was 4.2 GeV. The observed rate was found about half than calculated rate [25]. In analysis below we used a calculated rate as a conservative estimate of the background. In first measurement BigBite will be installed out of plane at polar angle 27°, at larger than nominal distance from the target, so the solid angle will be of 38 msr. The rates integrated over acceptance are shown in the Tab. 5.

field of 9 kG	e^-	$\pi^\pm$	proton
rate, MHz	0.05	1.30 x 2	1.20

Table 5: The singles rates in BigBite at luminosity $1 \cdot 10^{37}$ Hz/cm^2 for the configuration of first measurement.

In second measurement BigBite will be installed at 70° and used for detection of the soft protons with momenta 150-250 MeV/c. Ionization density for soft protons will be about 25 times that for electrons and pions of background. This allows to reduce the high voltage on the drift chambers and make them sensitive primerely to these slow protons. Other particles will contribute only to the rate of the scintillator counters which have high rate performance and segmentation. In second measurement BigBite information will be used only in off-line analysis. Table 6 shows expected particle rates in BigBite during second measurement.

field of 7 kG	$e^\pm$	$\pi^\pm$	proton
rate, MHz	0.8	7.5 x 2	7.5

Table 6: The singles rates in BigBite at luminosity $1 \cdot 10^{38}$ Hz/cm^2 for the second measurement.

2.6 Single rate in the neutron detector

In proposed experiment we will use the neutron detector N-200, which is under preparation for GEN experiment E02-013 [32]. In 2002 we built a 10% part of the full detector (20 neutron bars and 8 veto paddles) and used it for measurement of the single rates and trigger rates at position 8 m from the target and 25° from the beam line. Rates were found in reasonable agreement with DINREG based calculations [24].

Figure 7 shows the expected rate of the pions at different momenta, which contribute to the rate in N-200. The rate of neutrons is shown in Fig. 8.

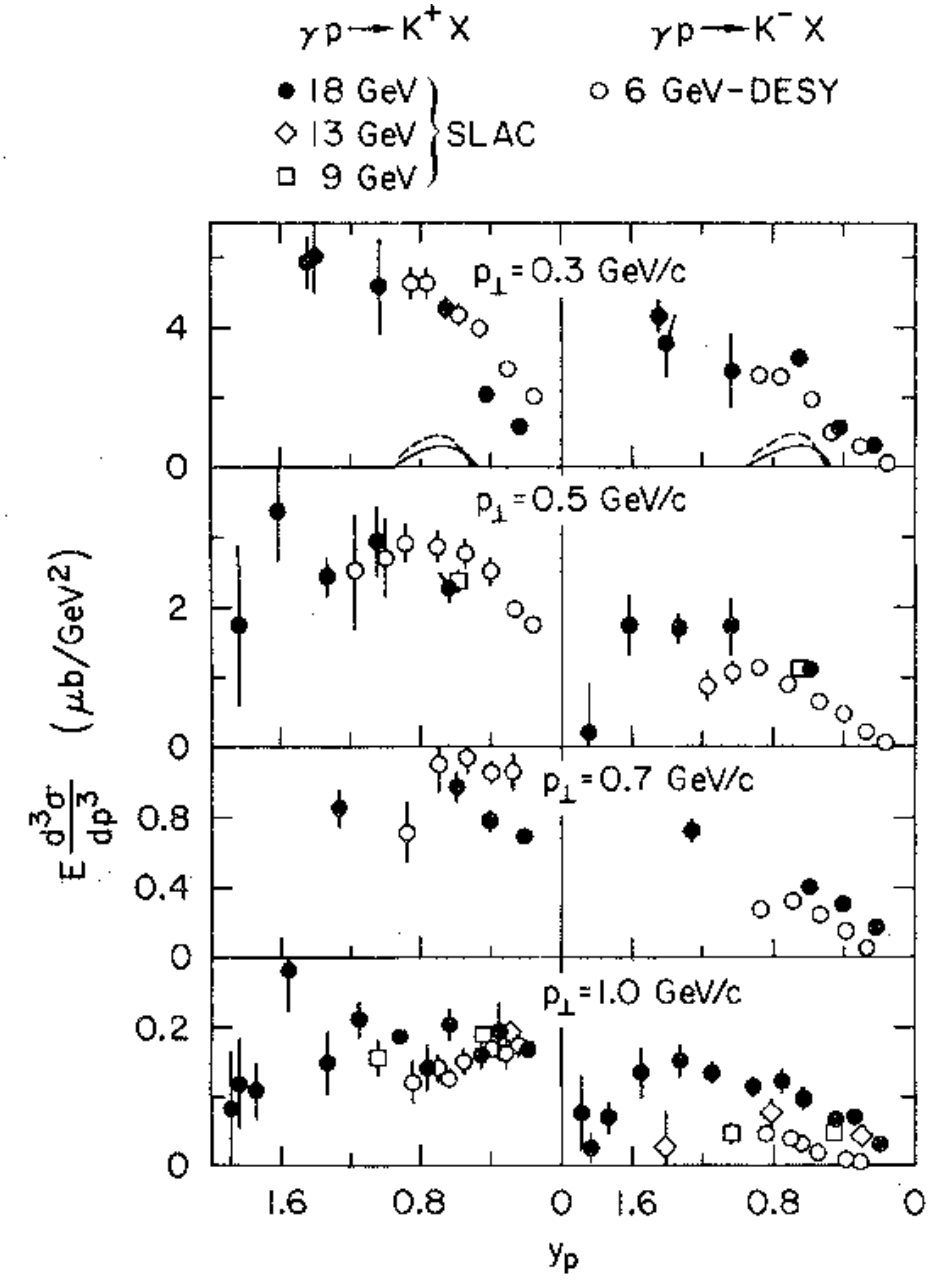

Figure 2: Inclusive kaon photo-production from the proton at different photon energy.

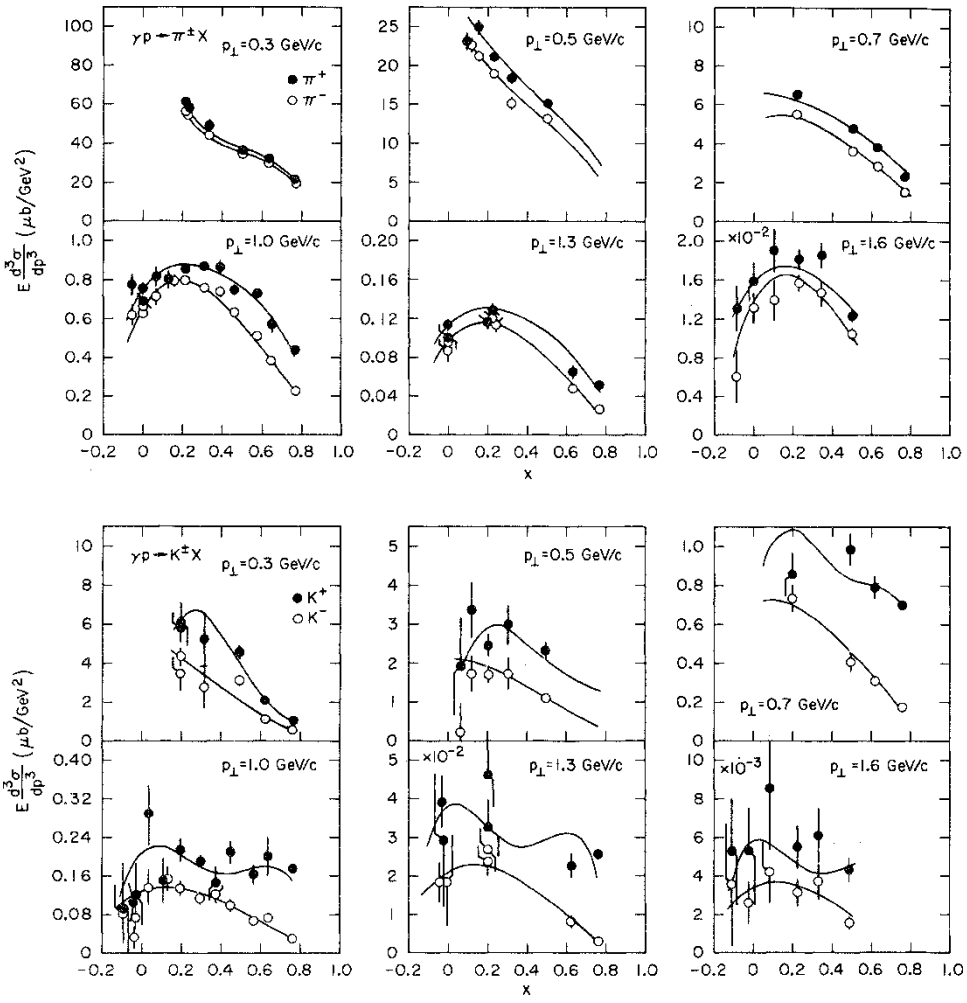

Figure 3: Inclusive pion and kaon photo-production from the proton [28].

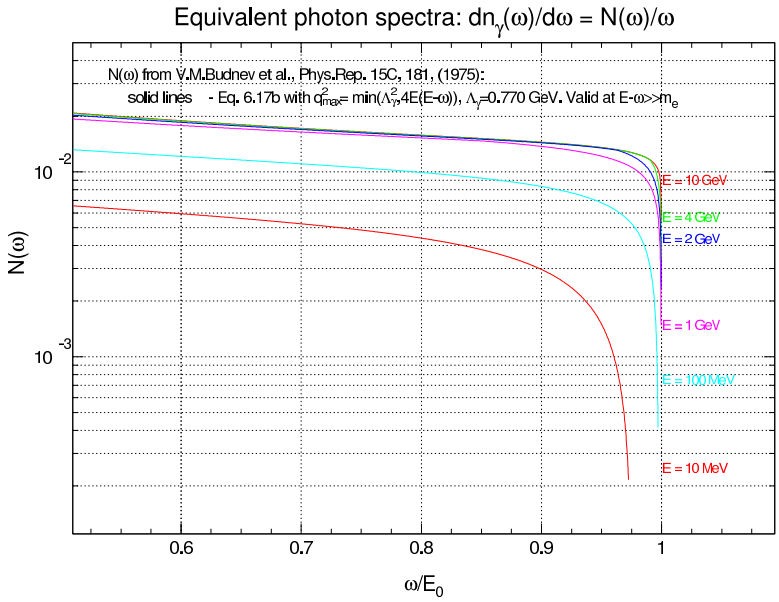

Figure 4: The photon spectra according to V. Budnev [31].

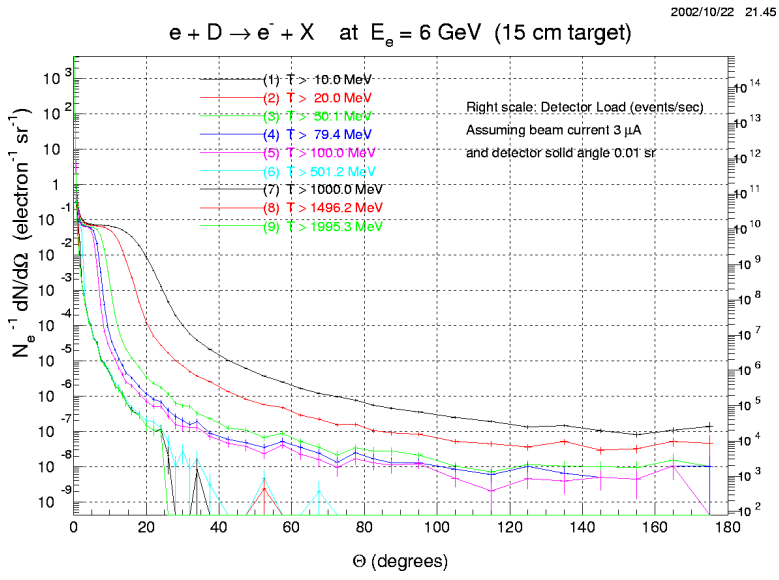

Figure 5: Electron rate at luminosity of 2.75×10^{37} Hz/cm^2.

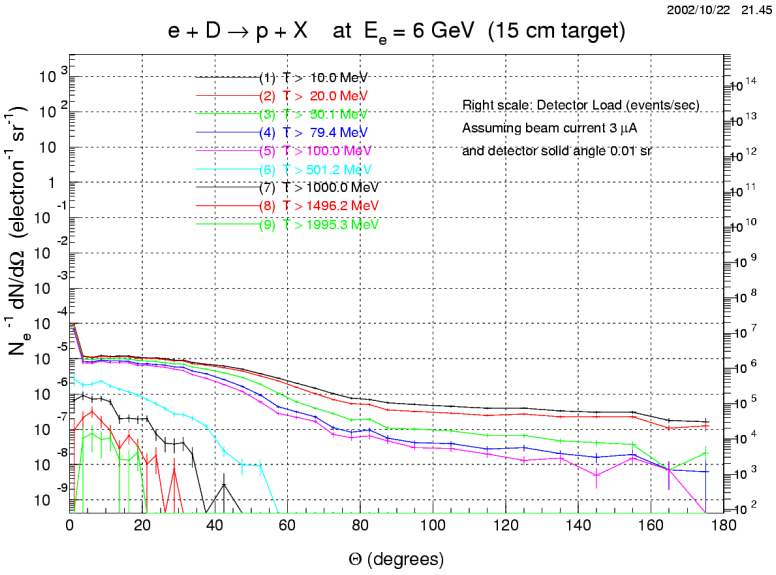

Figure 6: Proton rate at luminosity of 2.75×10^{37} Hz/cm^2.

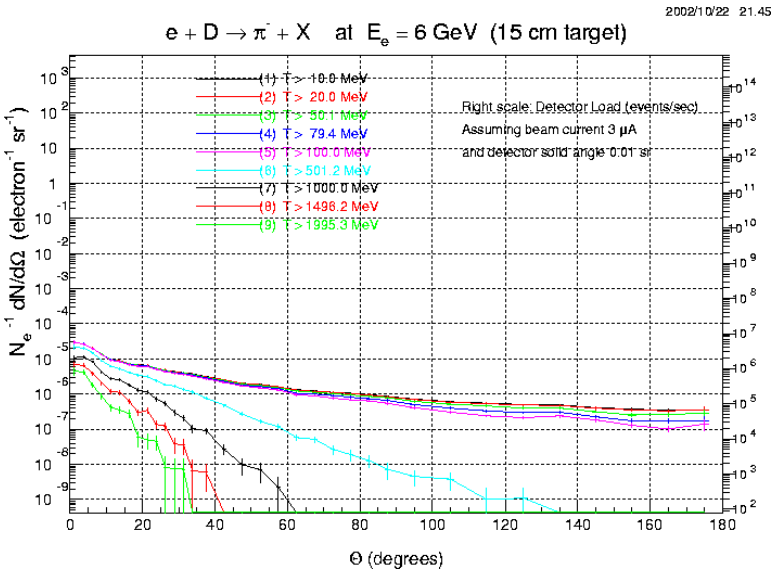

Figure 7: Pion rate at luminosity of 2.75×10^{37} Hz/cm^2.

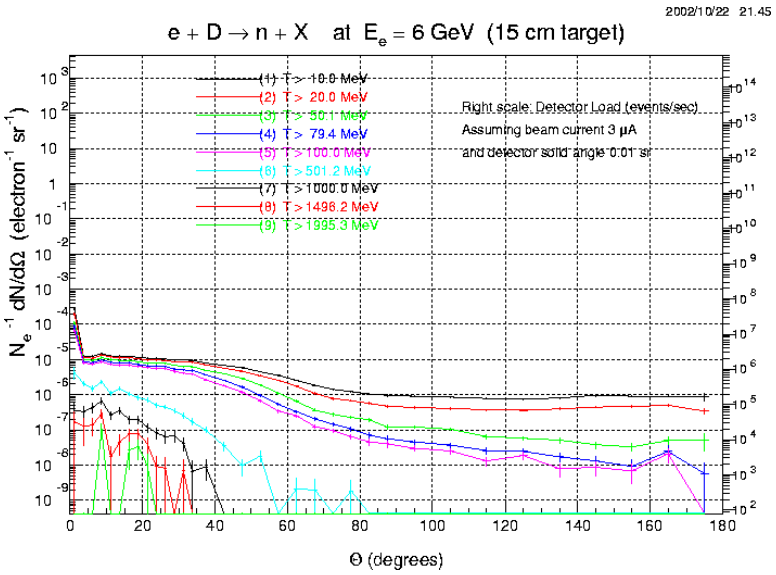

Figure 8: Neutron rate at luminosity of 2.75×10^{37} Hz/cm^2.

3 Experimental Setup

As illustrated in Figs. 9 and 10 this experiment will study the production of Θ^+ from deuterium target. The high energy forward going negative kaon will be detected in the High Resolution Spectrometer-left (HRS-left). In the first part of experiment the scattered electron will be undetected. Both decay products of Θ^+ will be detected and provide full information about Θ^+. The positive kaon will be detected in the BigBite and the neutron in the large neutron detector. In the second part of experiment the secondary electron will be detected in HRS-right. A soft proton will be detected in the BigBite to complete information about missing momentum and allow accurate reconstruction of the Θ^+ momentum and mass. These detectors are built or under construction for approved experiments. Kaon identification is already developed in HRS-left. It includes a time-of-flight system with resolution of 150 ps, threshold Cherenkov counters and Ring Imaging Cherenkov detector. For pion rejection in the BigBite the threshold Cherenkov counter with water radiator need to be constructed.

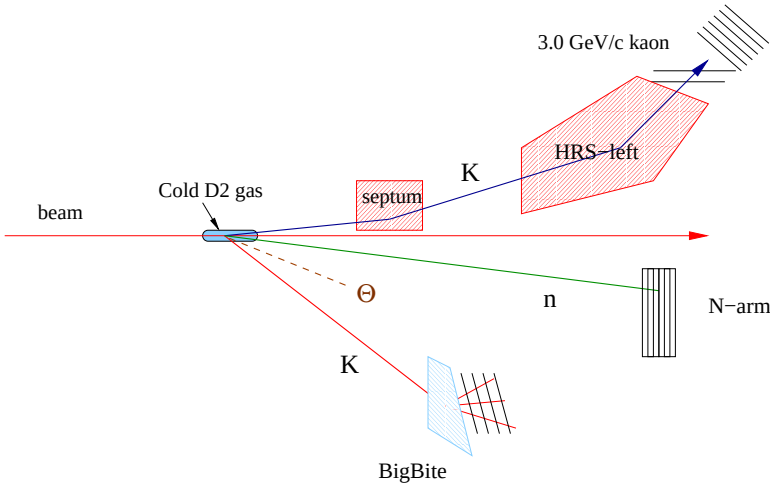

Figure 9: The experimental setup in the first part of experiment.

3.1 The CEBAF electron beam

The beam energy of 4.5 GeV will be used in the first part of this experiment. For the second part of experiment a higher beam energy of 6.0 GeV should give a better signal to background ratio. The time structure of the beam during first part of experiment will be similar one which was developed for the G0 experiment because it allows cleaner rejection of the protons.

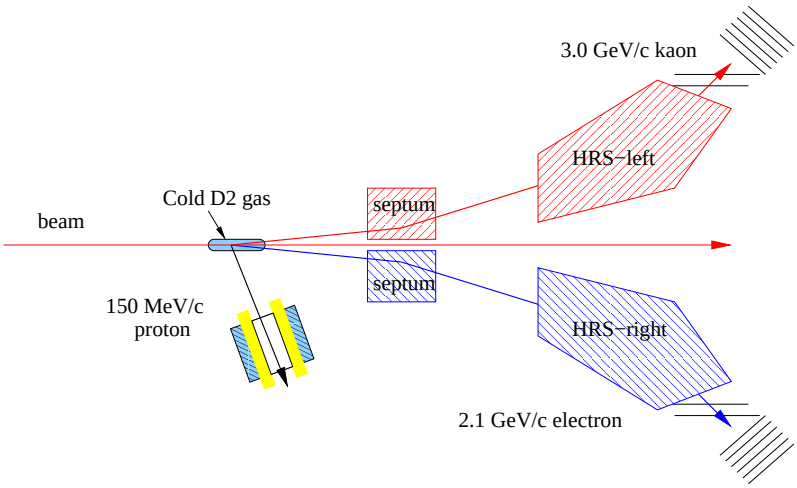

Figure 10: The experimental setup in the second part of experiment.

3.2 The cold gas deuterium target

The experiment will utilize the standard Hall A liquid hydrogen target system, but with the modernized target cell, shown in Fig. 11. It is a 50-cm long combined machined-soldered cell with 2 cm diameter and 25 μm wall thickness. The cell will be filled with deuterium at 28 K and pressure 2 atm. The density will be of 0.040 g/cm^2. Large length of the target allows to reduce gas density and pressure, which is important for reduction of the soft proton scattering in the gas and walls of the cell. Another important advantage of the long target is means of suppression of the accidental events.

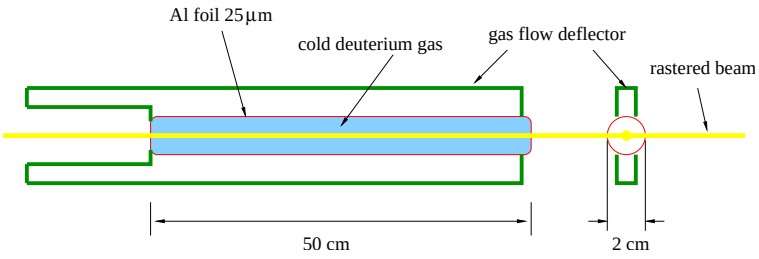

Figure 11: The concept of the long cold gas target.

3.3 The High Resolution Spectrometer-left

Basic parameters of the HRS-left are given in Table 7. Spectrometer has very good momentum and angular resolutions and moderate momentum and angular acceptances.

item	value
central momentum range, p_c	0.3-4.3 GeV/c
momentum acceptance, $\Delta p/p_c$	$\pm$ 4.5%
momentum resolution, σ_p/p	$1.1 \cdot 10^{-4}$
minimum angle for the central trajectory	6° with septum
solid angle for the point target	6.2 msr
coverage for scattering angle	3.1°
extended target acceptance, Y	$\pm$ 5 cm
θ_{disp} angular resolution,(rms)	1.5 mr
$\theta_{nondisp}$ angular resolution, (rms)	2.0 mr
target vertex Y resolution, σ_Y	1.5 mm
path from the target to the trigger	25.0 m
detector area (front chamber)	200 cm $\times$ 15 cm
trigger segmentation	16
time resolution, σ_{ToF}	0.15 ns

Table 7: The parameters of the HRS spectrometer.

3.3.1 The HRS-left particle identification

HRS-left has several means for particle identification specially for selection of high energy kaons. The PID can be used for on-line rejection of electrons and pions as well as for off-line selection of a very clean kaon event sample. There are two threshold Cherenkov counters in HRS-left called A1 and A2. The A1 is perfectly suitable for use in the trigger for rejection of the electrons and pion when kaon momentum up to 3.5 GeV/c. A1 radiator has refraction index n equal to 1.015 and A2 index n is 1.055. Effectiveness of these counters was shown during experiments E and in 2001 and 2002 (see Fig. 12 and Fig. 13). The detector package in HRS has two scintillator planes. Recently the old second plane in each HRS was replaced with new one, which time resolution (sigma) is about 150 ps per paddle. This will allow to realize identification of the beam bursts by using electron arm and measure the kaon ToF with 150 ps resolution on the flight path of 25 meters. For unique identification of the kaon the hyper-nuclei collaboration (Ejjjjj) constructed a Ring Imaging Cherenkov detector. It has liquid freon radiator and is perfect for kaon identification in few GeV momentum range. The on-line rejection of the electrons will be done by using signal from A1 aerogel Cherenkov counter and enhanced by a factor of 10 by use of the signal from the pion rejector - two layers shower detector, which is installed on HRS-left.

3.4 The High Resolution Spectrometer-right

The second HRS also with the septum magnet in 6° configuration will be used to detect the scattered electrons during the second part of experiment. Spectrometer has a vacuum connection to the scattering chamber in such setup. For electron identification HRS-right

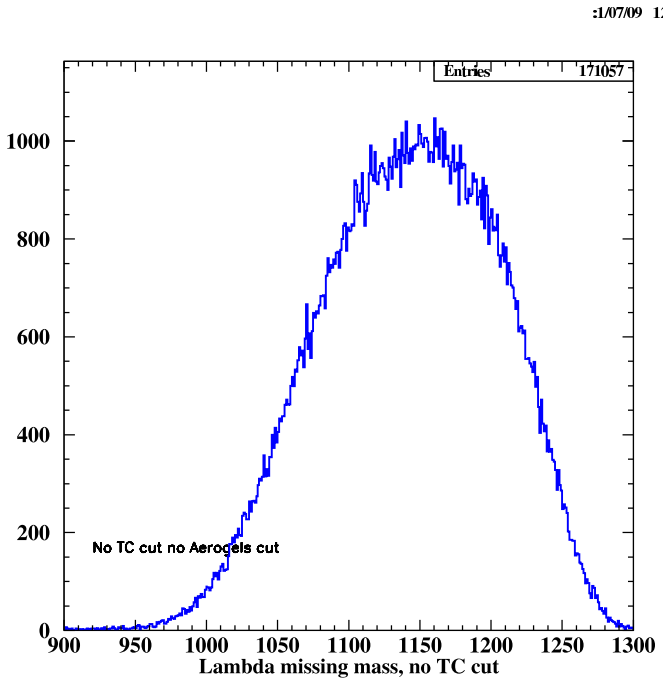

Figure 12: The missing mass spectra in H(e,e′K^+) measurement before applying any PID.

has a highly efficient gas Cherenkov counter and a preshower/shower lead-glass detector, which off-line combined rejection of the pions is about 10^5.

3.4.1 Operation with the septum magnet

First septum magnet was commissioned in July-August 2003 with HRS-right. Figure 14 shows the optic calibration data from the E97-104 experiment, which done by using this septum-HRS configuration in July-August 2002. Raw analysis of the momentum spectra is shown in Fig. 15. The reconstruction of the target vertex is shown in Fig. 16. These data confirmed that the HRS momentum and angular resolutions are the same as they are without septum.

3.4.2 The HRS-right particle identification

The PID will be used for on-line rejection of the negative pions as well for off-line analysis of the ToF. HRS-right has a gas Cherenkov counter with CO_2 radiator. On-line pion rejection factor of 20 and off-line factor of 200-300 was obtained. Preshower/shower detector of HRS-right can also provide on-line pion rejection of 10 and off-line about 100-300. New scintillator plane with time resolution of 150 ps allows identification of the beam bunch.

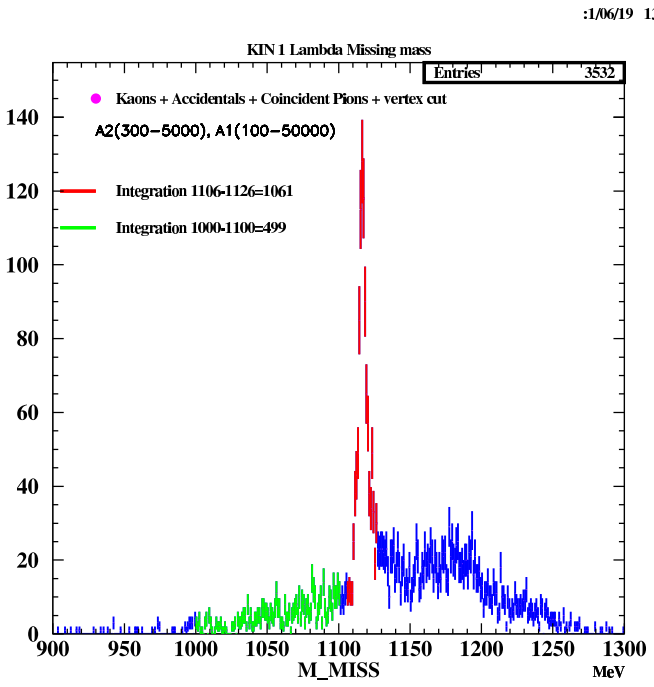

Figure 13: The missing mass spectra in H(e,e′K^+) measurement after all PID cuts applied.

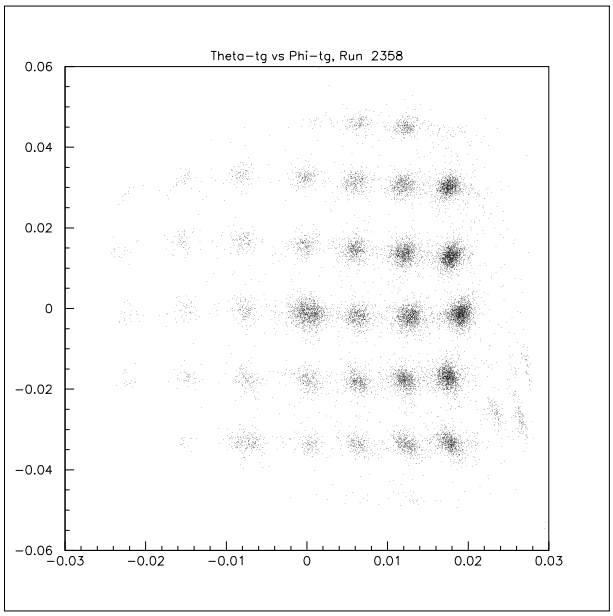

Figure 14: Sieve slit data for calibration of the optics.

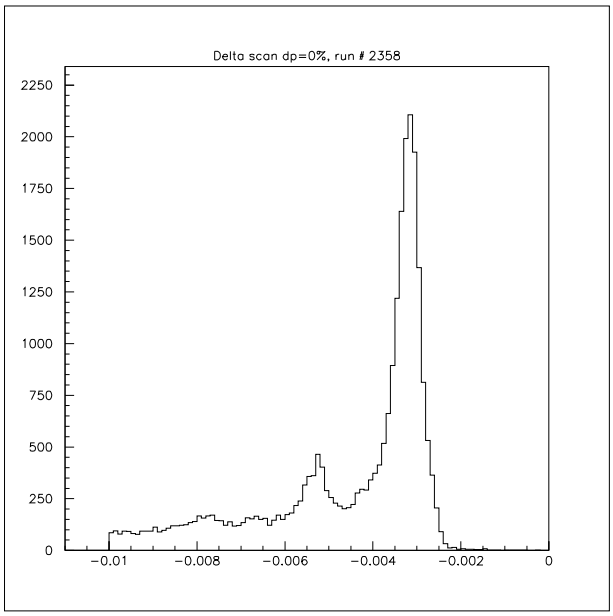

Figure 15: Momentum spectra for electron scattering form C-12.

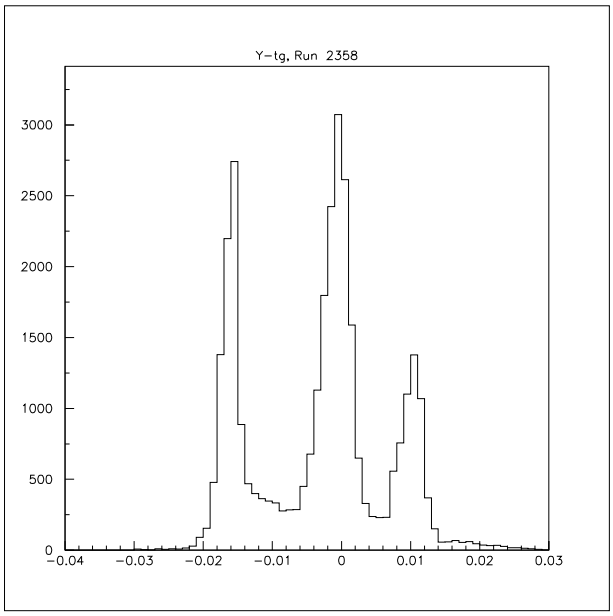

Figure 16: Target vertex reconstruction with septa.

3.5 The BigBite spectrometer

The BigBite spectrometer consists of a 20 ton dipole magnet and the detector system, which includes planes of drift chambers and trigger counters. The concept of such spectrometer was developed and realized at NIKHEF [33]. For operation in Hall A at larger luminosity the original detector system needs to be modified. The parameters observed for detection of a scattered electron are given in Tab. 8.

item	value
nominal momentum coverage (H=0.9 Tesla)	175-800 MeV/c
momentum resolution, σ_p/p	0.5-0.8%
solid angle for the point target	96 msr
solid angle for the extended target	86 msr
θ_{disp} angular resolution	5.0 mr
$\theta_{nondisp}$ angular resolution	2.5 mr
target vertex resolution, $\sigma_{_Y}$	5 mm
path from the target to the trigger	4.0 m
detector area (front chamber)	140 cm $\times$ 35 cm
trigger segmentation	24
time resolution	0.15 ns
Cherenkov counter segmentation (project)	48
size of the cell in drift chamber	$\pm$0.5 cm

Table 8: The parameters of the BigBite spectrometer.

3.5.1 The BigBite particle identification

The PID will be used for on-line rejection of the pions and slow protons. In off-line analysis the ToF, $\Delta E/E$, and momentum information will be used.

A threshold Cherenkov counter with water radiator (refraction index is of 1.33) will be used for pion rejection. Recently, HKS collaboration demonstrated that for kaon momenta up to 1.2 GeV/c the pion rejection factor is of 10^3, with a wave length shifter dissolved in the water to enhance light collection [37]. The water cell is made for each PMT, which allow to achieve high segmentation of the counter. The Time-of-Flight can be used for very effective particle ID when the detector has high segmentation and probability of two hits in a single beam burst is low. Such an approach was realized in the G0 experiment for detection of the recoiled protons and separation from the pions and electrons.

In the first part of experiment the BigBite will be used to detect kaons with the momentum 300-800 MeV/c. Kaon's time of flight is in the range of 15-30 ns. The value of the momentum and ToF will be used for identification of the positive kaon. In the second part of experiment the BigBite will be used to detect low momentum protons. They have time of flight in the range of 40-80 ns. The expected rate of 10 MHz with 24 segments in the trigger plane

leads to about 1 MHz per paddle. With 30 ns beam structure the probability of two hits in one paddle is about 3%. The time window of 30 ns between beam adjacent bursts allows unique determination of the particle speed and type because pions and electrons have much higher speed. Correlation of the speed and momentum will be used for suppression of the accidental hits. Segmented trigger plane for the BigBite was designed by GU [35] for set of experiments (Exxxx, Euuuu, Eiii) when the slow hadron should be detected in the BigBite. The plane consists of 24 E-counters and 24 ΔE counters. The thicknesses are 3 cm and 0.3 cm correspondingly. Each counter viewed by two PMT type XP2262. Figure **??** shows the picture of constructed and instrumented trigger plane. Figure **??** shows the ΔE - E correlation for protons, kaons and pions in momentum range of interest.

3.5.2 Momentum - Time-of-Flight and vertex correlations

For proton momentum as low as 150 MeV/c ToF information provide quite accurate determination of the particle speed. This information used in combination with coordinates in drift chamber allow dramatically improve angular resolution in dispersive direction. Correlation between ToF and momentum measured via deflection provide also the mean for rejection of the accidental proton hits. In present experiment two particles will be detected in HRSs and provide determination of the event vertex in target with accuracy of 1 cm. The vertex position allow in improve dramatically the angular resolution in horizontal plane, which is quite important for most accurate determination of the missing mass.

3.6 The neutron detector

The large neutron detector is under construction for GEN E02-103 experiment. It consists of 244 neutron bars and 184 veto paddles. They arranged in seven(five) layers with the iron converters and two veto planes. Figure 17 shows the schematic view of the detector cross section. Detector efficiency is about 35%, which includes significant loss of neutrons interacted in the front shielding or fired veto counters. Each neutron bar viewed by two PMT, so ToF resolution (rms) is of 0.3 ns. Because neutron energy in the proposed experiment much less than in GEN case the trigger threshold will be reduced from 50 MeV to 20 MeV and the front shielding will be reduced from 5 cm of Pb to 2.5 cm. The detector efficiency calculated in GEANT4 based code is shown in Fig. 18 for different threshold level.

The trigger scheme of the neutron arm based on summing of the signals from all counters of four vertical layers (total about 32 bars) is shown in Fig. **??**. Expected rate of the neutron arm trigger is about 0.7-1.0 MHz for threshold of 20 MeVee. The rate of individual PMT expected to be about 100 kHz with threshold of 5 MeVee.

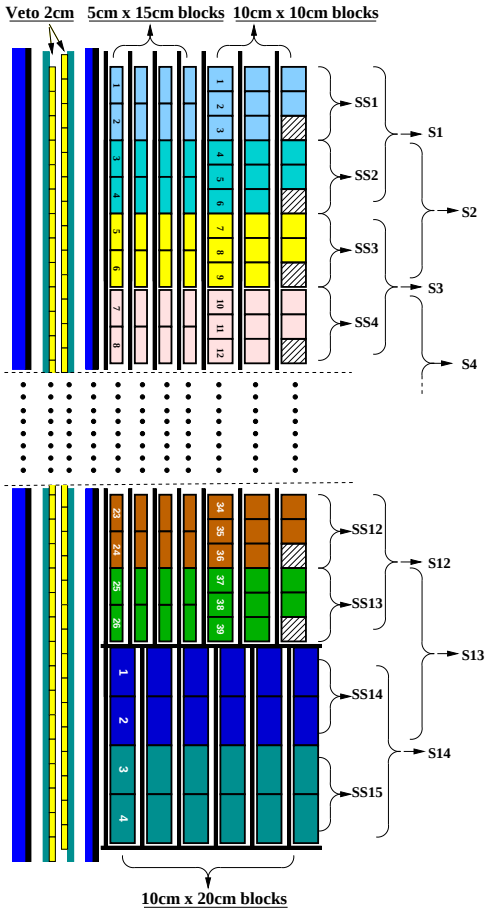

Figure 17: The scheme of the neutron detector.

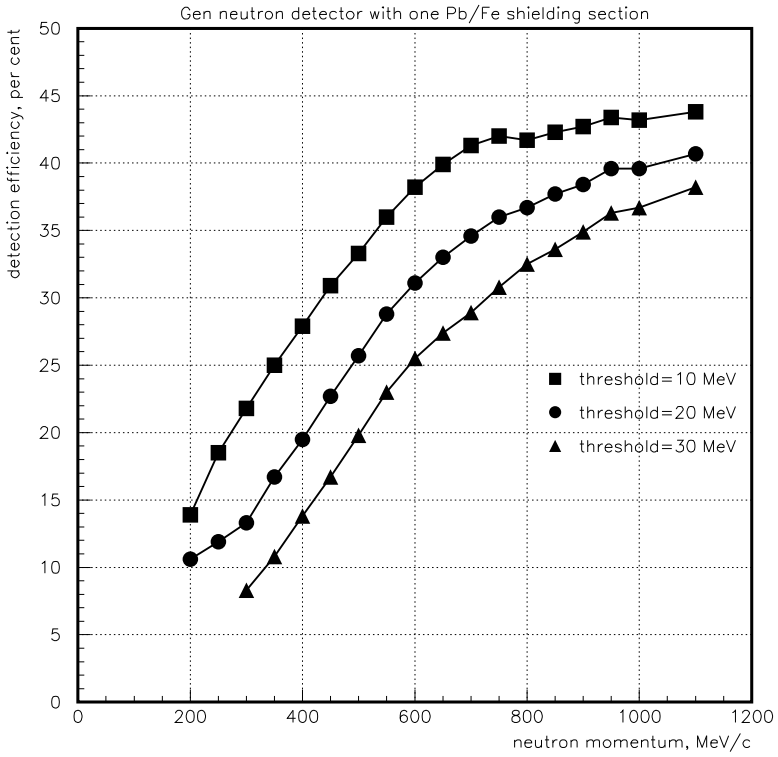

Figure 18: The efficiency of the neutron detector.

4 Proposed Measurements

There are several considerations in the base of present proposal. They are

- tagging on a high momentum kaon produced by a photon;
- a concept of post-target tagging;
- an assumption of the diffractive mechanism of Θ^+ production, which is considered in the calculations of the cross section for the n$(\gamma, K^- n K^+)$ [19, 20];
- a pair of high resolution spectrometers HRS in Hall A [34];
- a pair of novel septum magnets for HRS, which allow to detect particles for the central trajectory in spectrometer at angle of 6°;
- a large acceptance magnetic spectrometer BigBite [33], with high rate detector package is under construction for the GEN experiment [32];
- a large array of the neutron counters, which is also a part of the GEN experimental setup;
- a 50 cm long cold gas Deuterium target;
- the experimental data on forward photo-production of negative kaons [26, 27, 28].

The efficiency of **a tag on the negative kaon at large $x_{_F}$ and small $p_\perp^2$** presents the most important single consideration.

The post-target tagging approach, often used in hyper-nuclei experiment, is low Q^2 electro-production study photo-production processes. Because HRS spectrometer energy resolution (rms) is about $1.1 \cdot 10^{-4}$ such tagging has unique resolution. The effective flux of photons is also much higher than achievable with tagged of the real photon if an electron scattering angle is sufficiently small. In the first part of present experiment scattered electron will remain undetected. High energy forward negative kaon presents very important **tag**, which reduces dramatically the contribution of competing reactions into K^+-neutron event sample.

The mechanism of the Θ^+ state photo-production is unknown. However, it is logical to expect that it is similar to one for the $\Lambda(1520)$. The total cross section and a slope of t dependence are two parameters, which need to be measured. Cross section may also has $\sigma_{_{TT}}$ term, which can be estimated from experiment because of high degree of linear polarization of virtual photon.

Three separate measurements are proposed. The first will allow to observe a narrow Θ^+ state in an invariant mass spectra and angular distribution of the decay products. The second will allow to observe a narrow Θ^+ state in a missing mass spectra in the wide range of masses, to perform a most accurate measurement of the mass value and to find a role of a proton in the reaction mechanism. The third designed to search for Θ^+ state partners

in the antidecuplet and in the tensor multiplet, find them or put a very strict limit on the photo-production cross section.

All measurements will use a 50 cm long cold gas Deuterium (Hydrogen) target. In case of the Deuterium target three particles must be detected for complete reconstruction of the kinematics. The third arm will be a large neutron detector or second HRS spectrometer.

4.1 The invariant mass experiment

In this measurement we are going to study reaction n$(\gamma, K^- n K^+)$. The resonance decay products will be detected in the large neutron detector and the BigBite spectrometer. The concept of this measurement is shown in Fig. 9. In this approach the invariant mass resolution (FWHM) is about 3.5 MeV. If an actual resonance width will be found less than 3 MeV the experiment can be redone with HKS spectrometer [37] for detection K^+, when mass resolution will be in order of 2 MeV, however the counting rate will be less and angular coverage small.

4.1.1 The kinematics

HRS-left is selected for kaon detection because it equipped with threshold Cherenkov counters for pion rejection on trigger level [35] and top of the art RICH detector for identification of the kaon [36]. The value of kaon momentum of 3 GeV/c is followed from the photon energy and the angle of the spectrometer. The energy of the photon of 4 GeV leads to choice of 4.5-5 GeV electron beam energy because with higher beam energy the favorable high x_F become smaller and with lower beam energy the flux of equivalent photons is dropping (see Fig. 4). The direction of the Θ^+ particle is about 22° with distribution shown in Fig. **??**. Relatively small momentum of produced Θ^+ and low energy yield in its decay to K^+n channel leads to a large angle between K^+ and a neutron. Figure **??** shows the distribution of the events in polar angle between Θ^+ direction and K^+ in lab system. Because of kaon short life time we selected the region of the phase space with higher kaon momentum and lower neutron momentum as it is indicated in the same Fig. **??**. Forward direction of the Θ^+ leads to positioning of the detectors in place with high background rate. Specially if detectors are located in the same plane as negative kaon. We plan to put both detectors out-of-plane. The BigBite will be installed in the direction down by 15° and the neutron detector in the direction up by 22°. Such arrangement has relatively large angle between beam line and detectors (25-30°) and also large range of angle between Θ^+ momentum and decay products (due to favorable aspect ratio of the acceptance in BigBite and neutron detector) which is very important for determination of the resonance spin.

4.1.2 The calculation of acceptance

The Monte Carlo simulation of the setup was done in framework of GEANT-3. Figure **??** shows the event generated in the code. Figure **??** presents a distributions over the kaon momentum, the incident photon energy, the resonance momentum, the neutron momentum,

the positive kaon momentum, the correlation of the neutron and kaon momenta. The output of these calculations is a probability (P_a) to have all three particles (a negative kaon, a positive kaon and a neutron) in the acceptance of their arms. The value of P_a is of $1.7 \cdot 10^{-4}$ for configuration under discussion.

4.1.3 The calculation of the mass resolution

The event sample generated in previous MC study was used for analysis of the accuracy of the invariant mass reconstruction. The momentum resolution of the BigBite of 0.8% and time resolution of the Neutron arm of 0.4 ns were used in calculations. Figure **??** shows the simulated invariant mass distribution based on the detector resolution. The rms of the distribution is of 1.6 MeV.

4.1.4 The calculation of Θ^+ production rate

In calculation of the Θ^+ production rate we used the value of total photo-production cross section of 50 nb as an estimate based on information from CLAS expriment (60-160 nb) and the photo-production cross section from the article [20], which gaves it 130 nb at photon energy 4 GeV, it is in agreement with only one presently published result (200 nb at 2-2.5 GeV)[6]. We assumed 50% branching ration for decay to K^+n. When it used we assumed the resonance width (FWHM) equals to 3 MeV. The parameter for t dependence of the K^- angular distribution we used conservative value of 3 GeV^2, which is much less than known slope 6 GeV^2 for the $\Lambda(1520)$. We had found that for detectors of present proposal the resulting production rate is almost the same for the slope values between 2 and 6 GeV^2.

The calculations below of the production and background are made for an electron-nucleon luminosity $1 \cdot 10^{37}$ Hz/cm^2.

The photon-neutron luminosity was calculated as

$$\mathcal{L}_{\gamma n(eutron)} = \frac{N}{A} \cdot 0.015 \cdot \frac{\Delta E_\gamma}{E_\gamma} \cdot \mathcal{L}_{eN(ucleon)} \sim 3 \cdot 10^{-4} \cdot \mathcal{L}_{eN} \; = 3 \cdot 10^{33} \text{ Hz/cm}^2,$$

where E_γ and ΔE_γ are defined by the kaon momentum and its range accepted in HRS-left. Such value of $\mathcal{L}_{\gamma n(eutron)}$ is about 10^4 times higher than one can obtain with the real photon tagging. It leads to the production rate

$$\nu^{\Theta^+}_{\gamma,K^-nK^+} = \mathcal{L}_{\gamma n} \cdot \sigma^{\Theta^+}_{\gamma n} \cdot f^{HRS}_{\gamma,K^-} \cdot f_{nK^+} \cdot f^{decay}_{K^-} \cdot \eta_n \cdot f^{decay}_{K^+} \cdot b_{K^+n} \; = 33 \text{ events per day},$$

where $\sigma^{\Theta^+}_{\gamma n}$ is the cross section of 50 nb; the f^{HRS}_{γ,K^-} is a fraction of K^- associated with Θ^+ production within HRS angular and momentum acceptances, it is of 0.034; the f_{nK^+} is a fraction of Θ^+ events when both decay products are in angular acceptance of BigBite and N-arm detectors, f_{nK^+} is of 0.005; the $f^{decay}_{K^-} = 0.33$ is a surviving probability of K^- after 25 meter path in the HRS; $\eta_n = 0.35$ is a detection efficiency of the neutron; the $f^{decay}_{K^+} =$

0.40 is a surviving probability of K^+ after flight of 4 meter path from target to the BigBite trigger, and b_{K^+n} is a branching ratio for Θ^+ decay to K^+n, $b_{K^+n} = 0.5$. The actual rate $\nu^{\Theta^+}_{\gamma,K^-nK^+}$ may be higher or smaller if used cross section is not correct.

4.1.5 The singles and correlated rates

The singles rates in the HRS, the BigBite, and the neutron detector were calculated based on an analysis presented in Sec. 2. For the luminosity proposed for the first measurement the rates are presented in Tab. 9. Correlated rates due to real coincidence between π^- in

detector	momentum	rate, kHz	rate, kHz	rate, kHz
HRS-left	3.0 GeV/c	$\nu_e = 50$	$\nu_{pi^-} = 15$	$\nu_{K^-} = 0.35$
BigBite	>0.2 GeV/c	$\nu_e = 100$	$\nu_p = 700$	$\nu_{pi^\pm} = 600$
N-arm	A_{sum} >20 MeV	$\nu_n^{trig} = 200$	$\nu_{p,\pi^\pm}^{trig} = 1000$	

Table 9: The singles rates in the HRS, the BigBite and N-arm at electron-nucleon luminosity of 1×10^{37} Hz/cm^2 for the configuration of the first measurement.

HRS-left and electron in HRS-right was calculated from the intensity of virtual photon flux and hadron electro-production cross section (see Sec. 2). Such rate is about 150 kHz for electron-pion and 3.5 kHz for electron-kaon. Trigger rate will be on below 5 kHz due to on-line rejection of pions.

4.1.6 Trigger rate and event analysis

The trigger will use a coincidence between HRS and BigBite. On-line rejection factor of the electrons in HRS is about 500 based on combination shower detector and aerogel Cherenkov counter. On-line rejection of pions in HRS is about 100 based on aerogel Cherenkov counter. On-line rejection of pions and protons in BigBite expected on level of 10. With G0 beam time structure coincidence trigger will use time window of 100 ns and lead to comfortable accidental coincidence rate of 10 Hz.

Off-line analysis will allow to obtain higher rejection factor of pions and electrons in HRS by means of RICH, so event sample will have only negative kaon in HRS-left. Off-line analysis of BigBite data time-of-flight and water Cherenkov amplitudes will bring rejection factor to level of 1000 (see for example [37]). Off-line analysis of Neutron arm veto information will allow to reduce pion/proton rate by factor 50.

Remaining rate of accidental rate is 0.006 Hz. These events will make a background in invariant mass spectra distributed in 150 MeV wide region. The expected Θ^+ state production rate of 0.0005 Hz will be concentrated in region of 4.5 MeV. Such good ratio (peak/background of 3/1) provides sufficient insurance for the case if the actual photo-production cross section is even smaller than assumed in our estimation. The rejection factors used above are quite conservative also.

4.2 The missing mass experiment

In this measurement the resonance will be undetected, but observed in the missing mass spectra in the reaction D$(e, e'K^- p_{soft})$X . It requires detection of the electron, the negative kaon, and the proton. To achieve sufficient counting rate in this approach we rely on detection of a very soft proton. The number of such protons can be calculated from the spectrum function for the deuteron, which is shown in Fig. 19. For example the fraction of protons with momentum above 200 MeV/c is 6.8%. In addition to the events related to the spectator protons we estimated that similar number of events will be related to re-scattering of the proton and kaon and Θ^+ particle. The measurement of the proton spectra will allow to learn about reaction mechanism and may be even about the cross section of the proton-Θ^+ scattering. The technique for detection of the soft proton was recently developed for ChPT E01-014 experiment. It is based on BigBite spectrometer. ChPT experiment was designed for the proton momentum above 180 MeV/c. With proposed here a long cold gas target the threshold can be lowered to the level of 150 MeV/c. There are 13.5% protons with momentum above 150 MeV/c. We find that an optimum direction of the soft proton momentum, which can be used for BigBite together with two HRSs and septum magnets, is about 70 degree. We consider here the use of the BigBite, however for such slow protons simple time-of-flight can provide sufficient momentum resolution, so the combination of wire chamber and segmented ToF plane can be used. Because background study was done for BigBite we will consider its as a primary option for second measurement in this proposal.

An electron beam with current of 75 μA at energy of 6 GeV will be used. The density of gas will be adjusted to obtain the electron-nucleon luminosity of $1 \cdot 10^{38}$ Hz/cm^2. As was suggested above the negative kaon will be detected in the magnetic spectrometer HRS-left at central angle 6° with a septum magnet. The scattered electron will be detected in the magnetic spectrometer HRS-right at central angle 6° with the second septum magnet. The soft proton will be detected in BigBite spectrometer at central angle of 70°.

4.2.1 The kinematics

The central momentum of the kaon spectrometer will correspond to a quasi elastic production of the Θ^+ from neutron by a photon with energy of 4.0 GeV. Significantly larger than in first measurement electron beam energy leads to larger energy of the final electron and large momentum acceptance of the spectrometer. The scattered electron energy will be of 2.1 GeV, which corresponds to the range of the missing masses around 1.55 GeV. The BigBite angle value was optimized for better resolution of the missing mass within restricted space near the target.

4.2.2 The calculation of the acceptance

The Monte Carlo simulation of this setup was done in framework of GEANT-3. The results were confirmed by analytic calculations. Probability for the negative kaon to be in

angular acceptance of HRS-left in this measurement is about 5%, which is even larger than in the first measurement because the virtual photon direction is closer to HRS-left. Figure **??** presents a distributions over the kaon momentum, the scattered electron energy, the resonance momentum. The output of these calculations are the effective virtual photon flux, the probability of the negative kaon detection. The probability of soft proton detection with momentum above 150 MeV/c was found from effective solid angle of BigBite for extended target. For nominal length of the target 50 cm and BigBite angle of 70° the average solid angle is 60 msr. Fraction of protons in the deuteron with momentum above 150 MeV/c (P_{150}) was found from distribution shown in Fig. 19. We estimated from the value of K^-p elastic cross section that probability to find proton in the reaction H$(e, e'K^-)$X with momentum above 150 MeV/c can be higher than P_{150} by 30-50%.

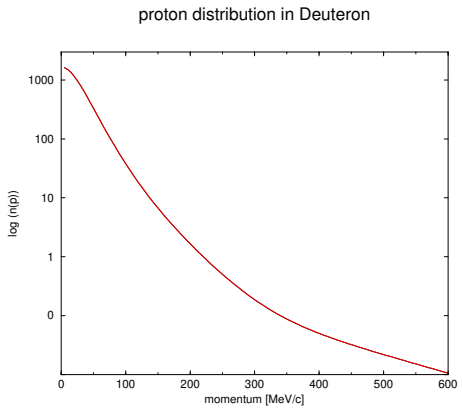

Figure 19: The proton spectra function in deuteron.

4.2.3 The calculation of the mass resolution

The event sample generated in MC simulation was used for estimation of the accuracy of missing mass reconstruction. The momentum and angular resolutions of the BigBite for soft proton was found from MC simulation, which includes all elements of the setup (see Tab. 10). For proton with momentum of 150 MeV/c a relative resolution is about 1.7%. The missing mass spectra is shown in Fig. 20. The distribution has rms of 1.5 MeV.

4.2.4 The Θ^+ events rate

The estimation of the production rate is quite similar to shown above for the first measurement. Detector configuration in the second measurement allow to use much higher luminosity. The calculations of the production and background are made for the electron-nucleon luminosity of $1 \cdot 10^{38}$ Hz/cm^2. By using standard electro-nuclear formalism (see Sec. 2) one can find that

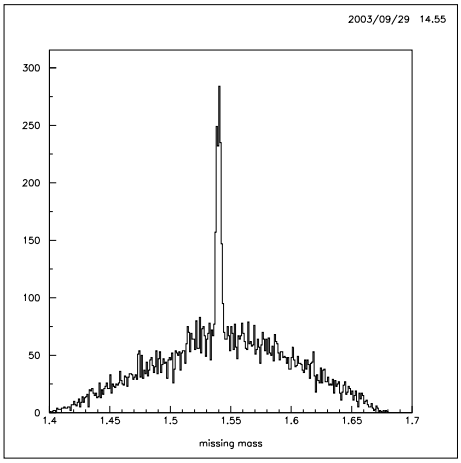

Figure 20: The missing mass spectra expected in the second measurement. The peak corresponds to the resonance width 3 MeV combined with an instrumental resolution (FWHM) = 3.5 MeV. Background level is an accidental coincidence at the luminosity of $1 \cdot 10^{38}$ Hz/cm^2.

momentum p, MeV/c	σ_p/p	$\sigma_{\theta,in\,plane}$	$\sigma_{\theta,out\,plane}$	z vertex resolution
140	1.9%	16.5 mr	13 mr	4.5 cm
160	1.5%	14.0 mr	10 mr	3.7 cm
180	1.2%	12.5 mr	8 mr	2.9 cm
200	1.1%	11.0 mr	6 mr	2.4 cm
220	1.0%	10.0 mr	5 mr	2.2 cm
240	0.9%	9.4 mr	5 mr	2.0 cm

Table 10: The resolutions of the BigBite spectrometer for soft protons in the proposed experiment.

$$\nu^{\Theta^+}_{e,e'K^-p} = \mathcal{L}_{en} \cdot \sigma^{\Theta^+}_{\gamma n} \cdot f^{HRS}_{\gamma^*,K^-} \cdot f^{decay}_{K^-} \cdot P_{150} \;=\; 30 \text{ events per day,}$$

where $\sigma^{\Theta^+}_{\gamma n}$ is the cross section of 130 nb; the $f^{HRS}_{\gamma^*,K^-}$ is a fraction of K^- associated with Θ^+ production within HRS angular and momentum acceptances, it was found from MC simulation of 0.049; the $f^{decay}_{K^-} = 0.33$ is a surviving probability of K^- after 25 meter path in the HRS; $P_{150} = 0.14$ is a probability for the proton in deuteron to have momentum above 150 MeV/c.

4.2.5 Trigger rate and event analysis

The trigger will use a coincidence between two HRSs. On-line rejection factor of the electrons in HRS-left is about 500 based on combination the shower detector and the aerogel Cherenkov counter. On-line rejection of hadrons in HRS-right is at least 10^4 based on use of a Gas Cherenkov counter and a shower counter. At luminosity of $1 \cdot 10^{38}$ Hz/cm^2 and 30 ns coincidence time window it leads to comfortable accidental coincidence rate of 30 Hz mostly

between kaon and electron. Off-line analysis of ToF allows to cut accidental rate by a factor of 15, to level when both particles produced in the same beam bunch. Analysis of the event vertex allow to cut accidental rate by an additional factor of 10-15 to the level of 0.1-0.2 Hz. Real coincidence rate of the electron and K^- is about 0.8 Hz.

The BigBite rate includes of 7.5 MHz soft proton rate and about 20 MHz rate of the pions and electrons. The time interval of 35 ns need to be considered for possible coincidence because of spread of ToF for our interval of the proton momenta. On this first step of analysis there is an accidental proton in 25% of eK^- events. The wire chamber rate will be defined mainly by protons due to reduced HV setting. The 200 ns time window of the back plane wire chamber and large amplitude pulse in the scintillator allow to identify proton track in the back wire plane and the scintillator. Correlation between time-off-flight and reconstructed momentum allow to select correct track in the front plane wire chamber. The event vertex reconstructed from HRSs tracks with accuracy (rms) of 1 cm and the vertex reconstructed from BigBite allow to reduce fraction of accidental events by a factor of 10-15 because of large length of the target. After such cuts the rate of accidental events will be of 0.02 Hz, which distributed over 200 MeV in the missing mass spectra.

4.3 The search for Θ^+ partners

In this measurement we propose to study reactions H$(e, e'K^-)$X and H$(e, e'K^+)$X. The goal is to find Θ^{++} partner and Σ° partner of Θ^+ state or put very strong limit on its photo-production cross section. Physics motivation for such search was discussed in the Sec. 1. The basic idea - **a tag on K^-**, as well as, the rate analysis are very similar to the one discussed above.

4.3.1 The kinematics and event rate

Only two HRSs are used in this measurement. Will be three settings. The kinematics for them are similar to the one used in previous measurement. The polarity of HRS-left will be positive in search for Σ^0 and negative in search for Θ^{++}. The momentum settings and other parameters are shown in Tab. 11. The rate analysis was done the same way as for the second measurement. Simulated missing mass spectra is shown in Fig. 21 if the cross section of the resonance is 5 nb with assumed mass of 1560 MeV. The resolution in missing mass in such measurement (FWHM) is about 1.5 MeV. In this case two days of data taking we can collect about 5500 events in the resonance peak. Such measurements will put an upper limit on production cross section on the level of 0.1 nb, which is of 1/500 of Θ^+ state photo-production cross section.

run	momentum HRS-left	momentum HRS-right	mass range
Θ^+	-3.0 GeV/c	-2.1 GeV/c	1450-1620 MeV
Σ^0	+3.0 GeV/c	-1.9 GeV/c	1560-1720 MeV
Σ^0	+3.0 GeV/c	-1.6 GeV/c	1700-1860 MeV

Table 11: The parameters of data taking in the third measurement.

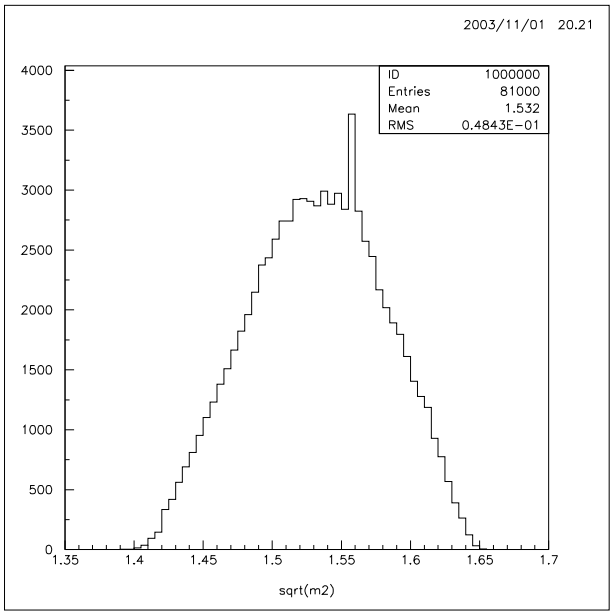

Figure 21: The missing mass spectra expected in the third measurement if photo-production cross section of the resonance is 5 nb. The peak corresponds to an instrumental resolution (FWHM) = 1.5 MeV and the resonance width (FWHM) = 3 MeV.

5 Expected Results and Beam Time Request

5.1 Parameters of the Θ^+ state

The width and the mass of the Θ^+ state will be investigated by two different approaches.

Assuming an accuracy of the absolute calibration of the beam energy (1.2 MeV for 6 GeV), which was obtained in Hall A [34], the knowledge of an angle for the central trajectories in HRSs (1 mr), and an absolute calibration of the HRS momenta on the level of 1 MeV/c we obtained an estimate of achievable accuracy for the Θ^+ mass about 1.3 MeV.

Assuming instrumental resolution (FWHM) of 3.5 MeV (see Sec.4) and statistics in the resonance of 400 events we found that accuracy of measurement of the width (Γ_{res}) will be dominate by the knowledge of the instrumental resolution. For conservative 25% accuracy on the instrumental resolution the $(\delta\Gamma_{res}/\Gamma_{res}) = 3.1\,MeV^2/\Gamma_{res}^2$ or 0.34 for $\Gamma_{res} = 3$ MeV. For example if the $\Gamma_{res} = 3$ MeV our expected results for Γ_{res} =will be 3 ± 1.0 MeV.

5.2 Search for partners of the Θ^+ state

The experiment will find the Θ^{++} or put the upper limit on photo-production cross section of Θ^{++} on level of 0.1 nb in the mass interval 1450-1620 MeV. Similar result for Σ^0 will be obtained in the mass interval 1560 - 1860 MeV.

5.3 Beam Time Request

The purpose of this experiment is to measure the parameters of the Θ^+ state and a search for its partners. Experiment will be done at two beam energy 4.5 and 6.0 GeV with current up to 100 μA.

Table 12 summarizes the beam time for data taking, We plan to do measurements in order M1, M2, M3. The M1 measurement is the most simple to prepare and it will allow to tune kinematical conditions for two triple coincidence measurements. The M2 measurement require installation of BigBite for detection of the soft proton. New equipment in this run is under construction for ChPT experiment E01-014. The M3 measurement needs more complicated installation and all detectors of GEN 02-013 experiment. If the full energy of 6.0 GeV will be not available slight change of the spectrometers momenta settings need to be done.

In total we request 33 days of beam-time to perform the proposed measurements.

kin. M#	type of measurement	current μA	energy GeV	time, hours
	HRS,BigBite calibration	10	2.0	4
	beam energy measurement	1	6.0	4
M1	partners search	100	6.0	120
M2	Θ^+ via missing mass	50	6.0	332
	beam energy	1	4.5	4
M3	Θ^+ via invariant mass	20	4.5	332
total				796

Table 12: The time allocation assuming 100% efficiency.

6 Conclusions

We request 796 hours of beam-time to measure the electro-production of Θ^+ resonance in two reactions and to conduct a search of the possible Θ^{++} and Σ^o partners.

Measurement of the width with instrumental resolution (rms) of 1.5 MeV will allow to find its actual value and enhance understanding of the nature of this exotic state.

Furthermore, it will be an investigation of the resonance parity, the spin, the form-factor and reaction mechanism, determination of the photo-production cross section.

We propose an experiment, which can establish the nature of the resonance or put very strong limit on its photo production coupling on order of 0.1% in comparison with the coupling of $\Lambda(1520)$.

Status of the equipment needed in the proposed measurements allow to realized it in time scale of one year. Additional resources may allow to reduce preparation time.

References

[1] D. Diakonov, V. Petrov, and M. Polyakov, *Z. Phys.* **A359**, 305 (1997); arXiv:hep-ph/9703373.

[2] T. Nakano *et al.*, [LEPS Collaboration], arXiv:hep-ex/0301020; PRL 91(2003)012002 1-4.

[3] V.V. Barmin *et al.*, [DIANA Collaboration] arXiv:hep-ex/0304040v2; Phys. Atom. Nuclei **66**, 1715 (2003).

[4] S. Stepanyan *et al.*, [CLAS Collaboration], arXiv:hep-ex/0307018; submitted to *Phys. Rev. Lett.* .

[5] V. Koubarovsky and S. Stepanyan, [CLAS Collaboration], in: *Proceedings of "Conference on the Intersections of Particle and Nuclear Physics (CIPANP2003), New York, NY, USA, May 19-24, 2003"*; arXiv:hep-ex/0307088.

[6] J. Barth *et al.*, [SAPHIR Collaboration], *Phys. Lett.* **B572**,127 (2003), arXiv:hep-ex/0307083.

[7] A. E. Asratyan *et al.*, submitted to Phys. Atom. Nuclei; hep-ex/0309042.

[8] A. Airapetian and M. Amarian [HERMES Collaboration], http://www-hermes.desy.de/notes/pub/trans-public-subject.html #EXOTICS

[9] C. Alt *et al.*, [NA49], arXiv:hep-ex/0310014.

[10] R. Jaffe and F. Wilczek, arXiv:hep-ph/0307341.

[11] M. Karliner and H. J. Lipkin, arXiv:hep-ph/0307243.

[12] S. Capstick *et al.*, arXiv:hep-ph/0307019.

[13] E. Shuryak and I. Zahed, arXiv:hep-ex/0311027.

[14] Fl. Stancu and D. O. Riska, arXiv:hep-ph/0307010.

[15] N. Auerbach, V. Zelevinsky, arXiv:hep-ph/0310029.

[16] S. Nussinov, arXiv:hep-ph/0307357.

[17] R. A. Arndt, I. I. Strakovsky, and R. L. Workman, arXiv:hep-ph/0308012; to be published in *Phys. Rev. C* **68**, (2003).

[18] E. M. Aitala *et al.*, *Phys. Rev. Lett.* bf 81, 44 (1998).

[19] M. Polyakov, private communication (2003).

[20] W. Liu and C. M. Ko, arXiv:nucl-th/0309023.

[21] Y. Oh, H. Kim, S. H. Lee, arXiv:hep-ph/0310117.

[22] P. V. Degtyarenko, "Applications of the Photo-nuclear Fragmentation Model to Radiation Protection Problems", Proceedings of the Second Specialist's Meeting on Shielding Aspects of Accelerators, Targets and Irradiation Facilities (SATIF2), 12-13 October 1995, CERN, Geneva, Switzerland, p. 67; P. V. Degtyarenko, M. V. Kossov, H-P. Wellisch, Chiral Invariant Phase Space Event Generator, I. Nucleon-antinucleon annihilation at rest, Eur. Phys. J. A **8**, p. 217 (2000).

[23] B. Wojtsekhowski, P. Degtyarenko, R. Lindgren, "A New Tool For Correlation Studies in Hall A at JLAB, JLab-TN-01-047", report on 5th Workshop on Electromagnetically Induced Two-Hadron Emission, Lund, Sweden, (2001).

[24] P. V. Degtyarenko, GEN collaboration meeting, 05/24/2003.

[25] P. V. Degtyarenko, GEN collaboration meeting, 10/24/2003.

[26] H. Burfeint *et al.*, *Phys. Lett.* **43 B**, 345 (1973).

[27] H. Burfeint *et al.*, *Nucl. Phys. B***74**, 189 (1974).

[28] A. M. Boyarski *et al.*, *Phys. Rev. D***14**, 1733 (1976).

[29] R. Feynmann, *Phys. Rev. Lett.* **23**, 1415 (1969).

[30] J. Benecke *et al.*, *Phys. Rep.* **188**, 2159 (1969).

[31] V. M. Budnev *et al.*, *Phys. Rep.* **15**, 181 (1974).

[32] G. Cates, B. Reitz, K. McCormick, and B. Wojtsekhowski, spokespersons, JLab experiment E02-013.

[33] D. J. J. de Lange *et al.*, *Nucl. Instr. Meth.* **A 406**, 182 (1998); D. J. J. de Lange *et al.*, *Nucl. Instr. Meth.* **A 412**, 254 (1998).

[34] J. Alcorn *et al.*, submitted to *Nucl. Instr. Meth.* **A** (2003).

[35] B. Wojtsekhowski *et al.*, in Hall A annual report, p.31 (2002).

[36] F. Garribaldi, private communication (2003).

[37] L. Tang *et al.*, HKS report for JLab readiness review, (2003).

[38] H. Walliser and V. Kopeliovich, submitted to JETP, hep-ph/0304058.

[39] K. Hagiwara *et al.Review of Particle Physics*, *Phys. Rev. D***66**, 010001 (2002); http://pdg.lbl.gov.

[40] Haiyan Gao, Bo-Qiang Ma, arXiv:hep-ph/0305294.